

Article

# A Finite-Element-Analysis-Based Feasibility Study for Optimizing Pantograph Performance Using Aluminum Metal Matrix Composites

Masengo Ilunga <sup>1</sup>  and Abhishek Agarwal <sup>2,\*</sup> <sup>1</sup> Department of Civil Engineering, University of South Africa, Pretoria 1709, South Africa; ilungm@unisa.ac.za<sup>2</sup> Mechanical Engineering Department, College of Science and Technology, Royal University of Bhutan, Phuentsholing 21101, Bhutan

\* Correspondence: agarwala.cst@rub.edu.bt; Tel.: +1-(802)-839-0488

**Abstract:** A pantograph is a key component on the tops of trains that allows them to efficiently tap electricity from power lines and propel them. This study investigates the possibility of using metal matrix composites (MMCs), specifically aluminum MMCs, as a material for making pantograph parts regarding the dynamics of the train's movement and external meteorological conditions. In this study, a computer-aided design (CAD) model is created using PTC Creo design software and moves to detailed finite element analysis (FEA) simulations executed by the ANSYS software suite. These simulations are important in examining how the dynamic performance of pantographs can vary. The incorporation of Al MMC materials into the structure of the pantograph resulted in significant improvements in structural robustness, with equal stress reduced by up to 0.18%. Similarly, aluminum MMC materials reduced the strain energy by 0.063 millijoules. The outcomes not only give a new perspective to the implementation of modern materials but also provide a breakthrough concept to improve efficiency and increase the service life of pantographs. This study marks a significant milestone in the theoretical development of essential train systems, furnishing eminent perspectives toward the tactical development of transportation infrastructure by suggesting new avenues for the smooth incorporation of smart materials in railway transportation, which would contribute to a more sustainable and reliable future.



**Citation:** Ilunga, M.; Agarwal, A. A Finite-Element-Analysis-Based Feasibility Study for Optimizing Pantograph Performance Using Aluminum Metal Matrix Composites.

*Processes* **2024**, *12*, 445. <https://doi.org/10.3390/pr12030445>

Academic Editor: Andrea Petrella

Received: 2 February 2024

Revised: 14 February 2024

Accepted: 19 February 2024

Published: 22 February 2024



**Copyright:** © 2024 by the authors. Licensee MDPI, Basel, Switzerland. This article is an open access article distributed under the terms and conditions of the Creative Commons Attribution (CC BY) license (<https://creativecommons.org/licenses/by/4.0/>).

**Keywords:** pantograph; metal matrix composites (MMCs); feasibility analysis; CAD model; FEA simulation; structural enhancement; aluminum MMC; equivalent stress; strain energy

## 1. Introduction

Pantographs are electro-mechanical devices placed on the top of electric trains in electrified railway systems. This combination of engineering precision with electrical elegance generates a vital symbiotic bond with the overhead tension wires, giving the locomotive the necessary energy (electric power supply) to run [1]. Historically, this symbiosis has played out in a one-wire setting, with the railway track humbly supplementing the return current. The power transmission dance in modern electric rail systems consists of a catenary and a parallel-running contact wire. The pantograph acts as an intermediate conductor and, through a spring-loaded mechanism, provides a proper and high-quality connection with the contact wire. This elaborate procedure is crucial for the smooth running of the train [2]. Nevertheless, the contact shoe roller slides vertically along the wire during the movement of the train and, thus, conducts an accidental symphony, giving rise to standing waves in the wire. Nonetheless, these harmonies are disturbed by electromagnetic wave interference, disrupting the smooth flow of the electrical current. The difficulties of harmonizing pantographs in proximity within specific systems are apparent. For high-altitude electric trains, where the pantograph would operate better at higher voltage levels and interfaces with overhead wires, reliability is a focal point. Although third-rail systems

have been recognized as reliable, the practical implementations usually favor pantographs. Pantographs are powered by compressed air from the braking system, with the spring acting as the extension mechanism, as shown in Figure 1.

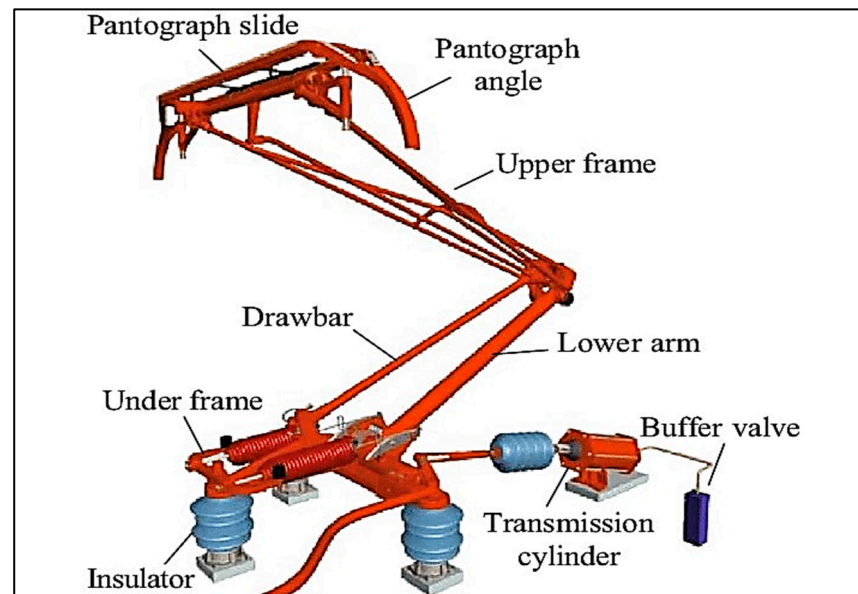


**Figure 1.** Pantograph structure [3].

Roof-mounted circuit breakers are crucial in high-voltage systems, where the air supply is used to neutralize the disruption from electric arcs. Pantographs, capable of appearing in both single-arm and double-arm forms, can be used for either full or partial electrification, enabling the fusion of electrical connections between contact lines and equipment.

The secure transmission of electrical energy is of paramount importance for mobile traction train applications, as well as residential installations [4]. The contact lines and pantographs, functioning as independent subsystems, play a crucial role in the general operation of the railway system [5]. Continuous mechanical linkages are crucial for sustained high efficiency; the system should be serviced periodically [6]. Thus, pantographs perform diverse functions depending on their configurations. The number of layers within the pantograph frame is the determining factor, resulting in a categorical classification that encompasses high-speed, regular-speed, DC, AC, single-layer, and double-layer pantographs [7]. In essence, pantographs can be classified into two groups depending on the presence/absence of spring-operated mechanisms. The objective of this study is to address the intricacies of pantographs, appreciating their fundamental role in the dynamic development of advanced high-speed rail systems and precision engineering. The spotlight moves to the examination of the existing body of knowledge compiled by scholars and engineers in this specialized field. Within the realm of multibody dynamics theory, Jiangwen Wang et al. [8] have provided a comprehensive explanation of the pivotal role of relative co-ordinates as the foundational framework for understanding the intricate dynamics of pantographs. This rigorous study methodically examined the quality of the connection between the two tension wires of a catenary system, employing thorough computation of the standard deviation (STD) of the dynamic contact force. The primary objective of this scholarly endeavor is to explore the consequences of structural modifications on the core design of a pantograph on the integrity of electrical contact. The overarching aim is to enhance the parameters governing high-speed rail systems and optimize the architectural blueprint of pantographs, thereby making a significant contribution to these evolving domains. Shimanovsky et al. [9] utilized the computational capabilities of MSC.ADAMS software to perform a detailed analysis of dynamic stresses at the intersection point between the pantograph and the overhead wire. This analytical journey revealed the temporal

fluctuations in the contact force exerted by the pantograph and its wire counterpart. Subsequently, a significant insight emerged from the computational analysis: a need for a thorough investigation into stress–strain equilibrium in the coal insert. Using the ANSYS program, this study leverages the finesse of FEA to determine the intricate contact interaction between the catenary wire and the pantograph. The intricacies of model construction extend to the use of various materials, including wire, anthracite, and steel liner. These computations expose the interconnections between corner stress levels and the breakdown of graphite in rectangular cross-sections. In the study by Yang Jia [10], it was clear that numerous researchers have diligently pursued this field. One of their focuses was a high-velocity inspection vehicle capable of achieving a remarkable speed of 378 km per hour and which featured an instrumented pantograph. The formulation of a numerical model for the pantograph–catenary system seamlessly integrates multibody dynamics with the absolute nodal co-ordinate formulation (ANCF). This comprehensive study delves into the nuanced differentiation between dynamic lift and contact force, conducting a meticulous comparative analysis that dissects disparities between numerical simulation and field-testing methodologies. The multibody dynamics model adeptly depicts the intricate motion of the pantograph within the high-speed railroad linking ‘Chengdu and Chongqing’, complete with an instrumented inspection/review vehicle cruising at 378 km per hour. The synthesis of field tests and numerical modeling yields a profound revelation: the current pantograph–catenary model exhibits remarkable accuracy when operating at the dizzying speed of 378 km/h. Nevertheless, computer simulations identify a deficiency in the trailing pantograph’s adherence to established assessment standards at this velocity. The remedy, as illuminated by this exploration, lies in adjusting both the double-pantograph interval and the emissary wire tension. Tripathi Utkarsh et al. [11] shed light on the pantograph engraving machine (PEM), a precision instrument designed to etch plates of wood, plastic, and mild steel with remarkable finesse. This study elucidates the intricate mechanisms that underpin the machine’s functionality, including the stationary bar mechanism. These mechanisms, in harmony with the tracer link, ensure precision in engraving. The creation of a precise duplicate of the pantograph engraving machine is entrusted to computer-aided design (CAD) software, such as AutoCAD and Pro-e, utilizing readily available components. While precision manufacturing is essential for high-performance components, design engineers often demonstrate creativity within limitations. Barpate et al. [12] explored wood engraving using a portable pantograph, expanding access. Their study detailed how the tracing mechanism could reproduce designs accurately and repeatedly. Seeking feasibility, investigators tested engraving pens guided by a manipulator to mass-produce copies. Portability, usability, and an affordable price point positioned this pantograph machine for diverse makers. Its lightweight construction accommodated mobility between projects. Relative to more complex tools, designers prioritized dependability through the engraving mechanism to address production challenges. The pantograph’s flexibility demonstrated the potential for manual skills to adapt industrial techniques accessibly. The study by John Morris et al. [13] provided a thorough literature review and pioneering effort to replicate patterns using a focused methodology. Their investigation addressed whether incorporating brief neutral elements could benefit outcomes in the UK setting. Employing a novel finite element analysis, the researchers dynamically simulated the interplay between overhead electricity lines and the pantograph collector to test this. Most previous research was focused on static scenarios, but this work made use of computational modeling to quantify dynamic interactions in varying situations. Information from their fine-grain simulation can provide the direction as to where streamlined implementation of neutral building blocks could increase concentration without jeopardizing other considerations. The research attempts to answer the question of whether neutral elements contribute positively to performance indicators regarding Great Britain. The investigators use a specific finite element analysis process for the dynamic modeling of the interaction between OCL and the pantograph. Based on the neutral component obtained from DCT and physical characteristics, an assembly of active elements within a pantograph/OCL simulation model

is meticulously conducted. The validation of the outputs of the entire simulation, which focuses on the neutral section, relies on meticulous test data.

This distinctive approach is leveraged to scrutinize the performance of the neutral section and ascertain its responsiveness to different structural components. Paweł Zdziebko et al. [14] embarked on an ambitious journey to explore the intricate relationship between the catenary and the pantograph through a co-simulation approach. The examination of both systems is predicated on an innovative co-simulation method for data exchange between pantograph and catenary models, all underpinned by a multi-domain approach. The depiction of the slider and dropper components of the pantograph in the context of a nonlinear (FEA) finite element catenary model takes the spotlight. The multibody model introduces the complexities of friction forces and suspension springs, adding a layer of intricacy to the narrative. The dynamic modeling of the pantograph further taps into the fluid–structure interaction technique to assess the impact of wind on its aerodynamic forces. A comprehensive study is embarked upon to scrutinize the correlation between the catenary and the pantograph, all while considering the magnetic forces acting upon the pantograph, the locomotive’s tilt, and the ensuing vertical vibrations. Zhenfeng Wu et al. [15] ushered in a new era by harnessing computational fluid dynamics (CFD) software to calculate the aerodynamic drag on a variety of pantograph fairings and structures. This study positions three distinct pantograph fairings under the limelight, each fulfilling specific roles. Through a comparative analysis, the team unveils the nuances of aerodynamic drag, surface pressure, and airflow within the intricate dance of a flow field. It emerges that the ellipsoid pantograph fairing stands as a paragon of performance, with the guiding surface following closely. In stark contrast, the double-arch fairing finds itself at the rear of the pack. The elliptical pantograph fairing emerges as the harbinger of the lowest total aerodynamic drag, followed by the double arch and guiding surface, each in their respective order.

The implementation of this pantograph enclosure results in a notable reduction in aerodynamic drag, amounting to 56.7 percent within the speed range of 0 to 300 km per hour. Sidorov et al. [16] categorized pantograph models into three distinct groups: reduced mass models, rod models, and CAD models. This research aimed to recognize a dynamic pantograph model for high-speed electric transportation systems. Experimental measurements of contact pressure at a catenary contact segment are compared with estimations derived through computational methods. Dongli Song et al. [17] conducted a study to assess the efficacy of a pantograph–catenary system by analyzing its contact area. The introduction of wear and other causes contributes to a stochastic element, while the irregularity of the contact strands gives rise to a periodic component. These phenomena are generated, among several other factors, under the influence of gravitational forces. Periodic and low-frequency random anomalies often lead to an increase in the amplitude of the contact force in regions where the peak wavelengths are shorter than the length, span, or spacing of the tension droppers. The key component that contributes to the decline in the system’s dynamic performance is a random irregularity observed at high frequencies, which, in turn, affects the amplitude across all frequencies. A negative association has been seen between the size of the shape parameter and its dynamic performance. The amplitude of contact wire irregularity and the cutoff value of the contact strip form parameter  $A$  may be determined by the calculation of contact force eigenvalues, which are dependent on frequency. The utilization of the threshold specified in this study may be employed by information and intelligent health management systems for high-speed rail to examine various components and ascertain the necessity of maintenance.

Within the scope of this study, a conspicuous research gap emerges, centered on the utilization of metal matrix composite (MMC) materials for pantograph design and a comprehensive evaluation of their mechanical characteristics. The existing literature lacks substantial insights into the potential advantages and limitations of integrating MMCs in pantograph applications, particularly concerning their response to multifaceted mechanical stresses encountered in real-world operational conditions. In response, we formulate a research hypothesis that the integration of MMC materials in pantograph construction

will yield enhanced mechanical performance and durability, making them a practical and advantageous choice for diverse transportation systems as per aspects considered in other transportation applications by [18,19]. The core objective of this research hypothesis is to elucidate the potential enhancements in mechanical properties and durability achievable through the application of MMC materials in pantograph design.

To effectively address the research gap and scrutinize the proposed hypothesis, a set of research questions has been devised:

1. What are the fundamental mechanical properties of MMC materials and how do they compare with the traditional materials typically employed in pantograph construction?
2. How does the integration of MMC materials impact the structural integrity and performance of pantographs under varying loading conditions?
3. What mechanical insights can be gained from the comparison of MMC and conventional cast-iron pantograph and how do these findings inform potential benefits and constraints associated with the adoption of MMC materials in pantograph design?
4. Considering the inherent limitations, how does the performance of MMC-based pantographs measure up against conventional pantographs when subjected to the real-world mechanical stresses encountered in transportation systems?

It is essential to recognize the shortcomings inherent in this study, which include assumptions regarding model simplifications and FEA simulation. This study focuses mainly on mechanical characteristics encountered in pantograph operation, neglecting complex dynamics and operational factors found inherent to real-life transport systems.

In addition, the results can be specific to the MMC materials used and the loading conditions chosen, which may require further investigation. This research addresses the basic issue of an urgent need to make a complete assessment of the viability and benefits associated with MMC materials being used in designing pantographs within transport systems. In these systems, the pantographs play crucial roles as they possess immense structural integrity and can withstand high mechanical stresses.

Thus, a holistic discussion on the benefits and disadvantages of mechanical properties of MMC pantographs should come first in the decision-making process. The purpose of this study is to address the current knowledge gap and produce information that facilitates smarter transport systems. Therefore, this research seeks to achieve analysis of the viability of MMC materials in pantograph design through CAD modeling with Creo and FEA simulations using the ANSYS program.

## 2. Materials and Methods

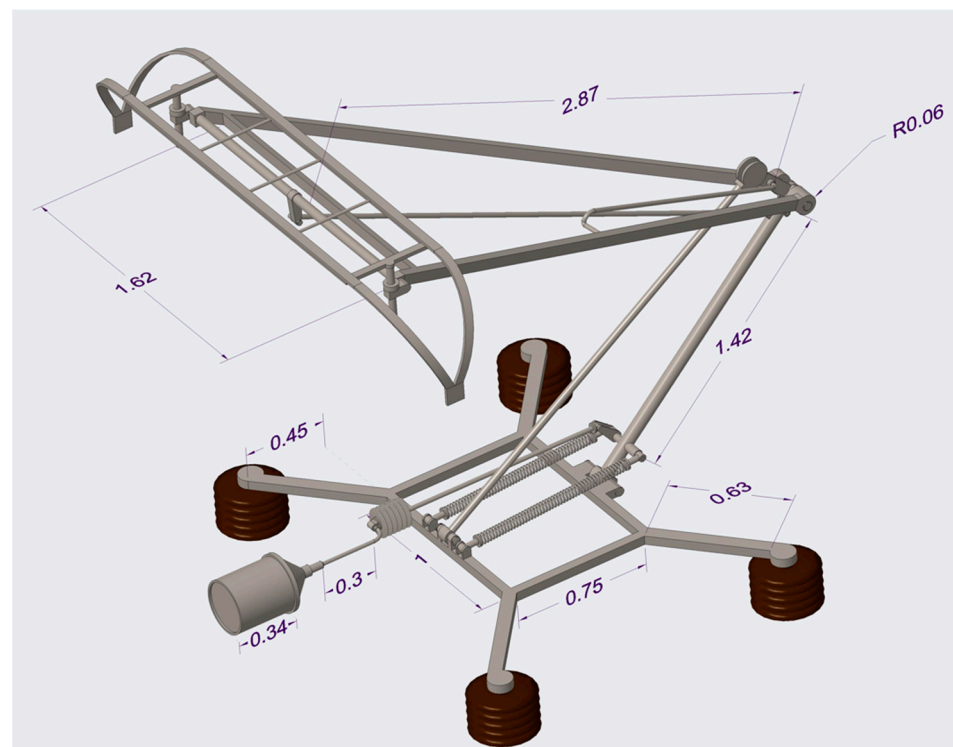
The methodology used in the structural analysis of the pantograph is a very organized process that consists of CAD modeling, creating the mesh, and applying the boundary conditions, followed by final comprehensive postprocessing [20]. As regards the structural analysis, the selected methodology is a static analysis model that is specifically developed to check the behavior of the pantograph components under a constant load condition, where the applied load is kept constant over time. Such a deliberate decision allows in-depth investigation of the long-term response of the structure to the applied forces, giving a deep understanding of its performance under service loads. Because of its ability to provide analytical accuracy, an isotropic material model has been used, adapted to both cast iron as well as aluminum metal matrix composite (Al MMC) material. The chosen mode is consistent with the intrinsic properties of these materials, thus allowing a more accurate depiction of their behavior. The isotropic model, in which the material properties are considered homogeneously in all directions, improves the accuracy and relevance of the structural analysis, offering a substantiated and holistic approach to assessing the dynamic responses of the pantograph components. The properties of these materials are provided in Table 1.

**Table 1.** Properties of the considered material (isotropic model).

Property	P100/AZ91C Mg MMC [21]	Cast Iron [22]
Modulus of Elasticity (MPa)	342,500	110,000
Poisson's ratio	0.295	0.28
Density (kg/m <sup>3</sup> )	2500	7200

### 2.1. CAD Modeling and Error Scrutiny

The first step in the structural analysis journey is to develop a comprehensive computer-aided design (CAD) model of the pantograph. This model is the working framework for subsequent phases. When the CAD model is created, it is then thoroughly evaluated within and through the ANSYS Design Modeler. This scrutiny is aimed at detecting and rectifying geometric errors, surface imperfections, or any other errors related to the model's surface characteristics. The designed pantograph model, meticulously examined and refined, takes its form, as exemplified in Figure 2. The model is designed in Creo and all approximate dimensions are in meters.

**Figure 2.** CAD model of the pantograph.

### 2.2. Mesh Generation and Complexity Handling

A pivotal step in the process is the discretization of the pantograph model based on its geometric complexity. To translate the model into a format that can be effectively analyzed, mesh generation becomes imperative [23]. The meshing process adopts tetrahedral element types, ensuring a fine-sizing strategy and normal inflation where necessary. The result is an intricately meshed model of the pantograph, unveiled in its entirety in Figure 3.

This meshed model is a testament to the painstaking detail invested, comprising a substantial assembly of 63,911 elements and an impressive 114,521 nodes.

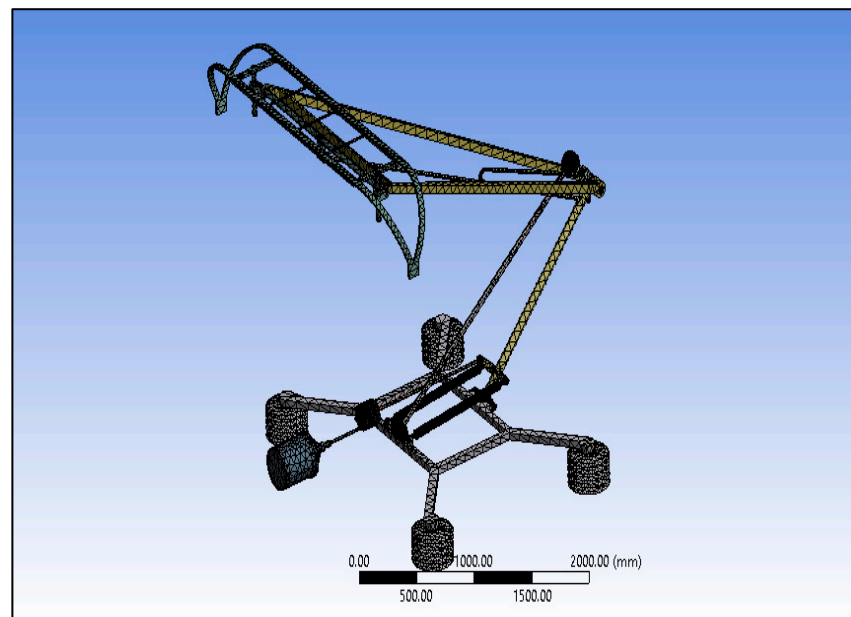


**Figure 3.** Meshed model of the pantograph.

### 2.3. Imposition of Structural Boundary Conditions

The essence of the structural analysis hinges on the imposition of rigorous structural boundary conditions. In this phase, the pantograph model is subjected to displacement support, primarily focused on the insulator region.

Simultaneously, a downward force of precisely 15 Newtons is applied to the pantograph slide, as vividly illustrated in Figure 4 [24]. These boundary conditions encapsulate the real-world scenarios and operational stresses that the pantograph endures.

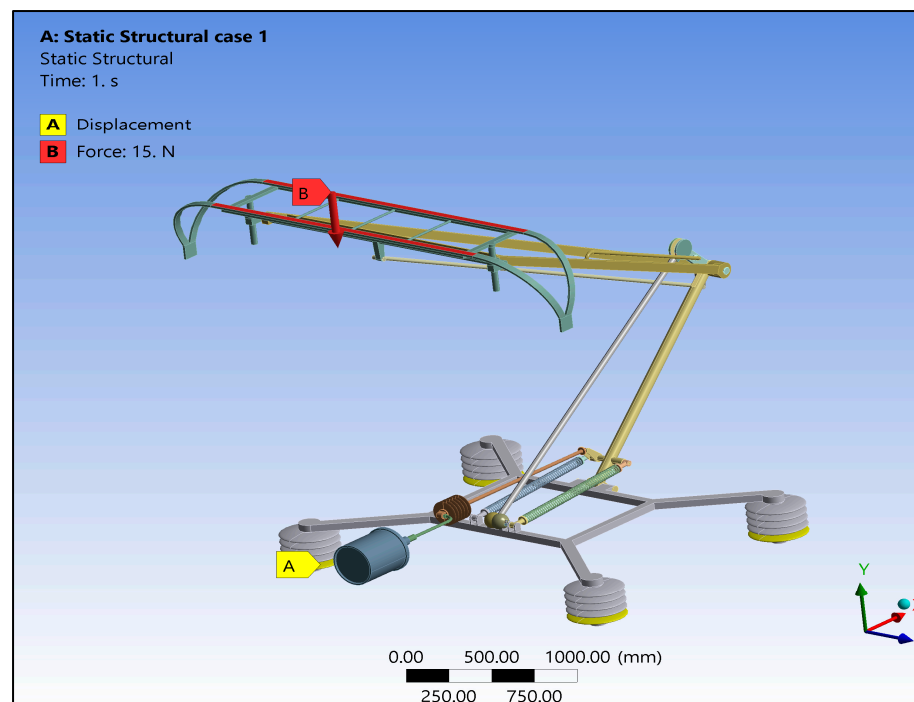


**Figure 4.** Structural boundary conditions applied to the pantograph model.

## 2.4. Simulation Scheme

With the structural boundary conditions firmly in place, the simulation phase is initiated, where the ANSYS 2023 R2 software rigorously computes the stress distribution and deformation patterns within the pantograph. The outcome of this comprehensive analysis unveils invaluable insights into the structural integrity and performance of the pantograph under the defined loading conditions.

This methodological approach, characterized by accuracy and carefulness, enables the study to reveal complex pantographic responses, along with mechanical attributions that provide insight into its actual functioning.

## 3. Results

The FEA sheds light on the structural behavior of cast-iron pantographs, as well as their counterparts made from Al MMC and P100/AZ91C Magnesium Material. The analysis of deformation and equivalent stress distribution is detailed and significant aspects of the mechanical properties under loading are revealed.

### 3.1. Equivalent Stress Distribution in the Cast-Iron Pantograph

Figure 5 below shows a plot diagram for the cast-iron pantograph, through which we can derive an equivalent stress distribution. It very clearly presents the greatest value of equivalent stress concentration at the point where the upper frame and drawbar meet. The highest equivalent stress reading in this analysis is measured at 5.8034 MPa.

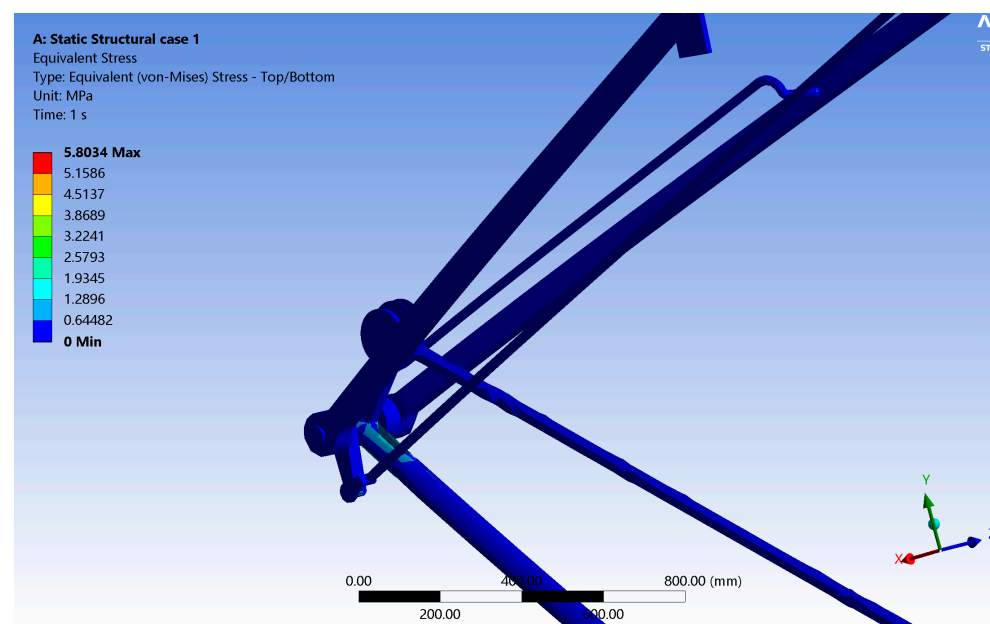


**Figure 5.** Equivalent stress graph obtained on the cast-iron pantograph.

Promisingly, the normalized stress shows a high level of consistency in other regions depicted by peaceful areas colored blue. The maximum equivalent stress obtained for the cast-iron pantograph is 5.8034 MPa, which is in close agreement with the results in the literature [24].

This uniformity underscores the material's ability to withstand stress throughout the structure. Table 2 displays the results of the grid independence test refinement, highlighting the correlation between the number of generated elements and the resultant equivalent stress values, measured in MPa. This test constitutes a crucial phase in the analysis process, intended to ascertain the dependability and consistency of finite element analysis findings. Through a systematic variation in element numbers, a meticulous examination of their

influence on equivalent stress levels is conducted, providing essential insights into the precision and convergence of the computational model.

**Table 2.** Grid independence evaluation.

Number of Elements	Equivalent Stress (MPa)
62,225	5.72
62,547	5.75
63,864	5.84
63,911	5.85

The table incorporates not only the fluctuations in equivalent stress but also includes specific details regarding the number of elements considered at each stage of the analysis. This comprehensive presentation ensures a clear and informative representation of the results, facilitating a deeper comprehension of the grid independence examination.

### 3.2. Total Deformation in the Cast Iron Pantograph

Figure 6 provides a comprehensive view of the total deformation plot for the cast-iron pantograph. It draws attention to the maximum deformation, which is prominently observed on the pantograph slide, registering at a magnitude of 1.5353 mm, as is evident in the striking, red-colored region. This deformation analysis underscores the structural integrity of the cast-iron pantograph under the applied load.

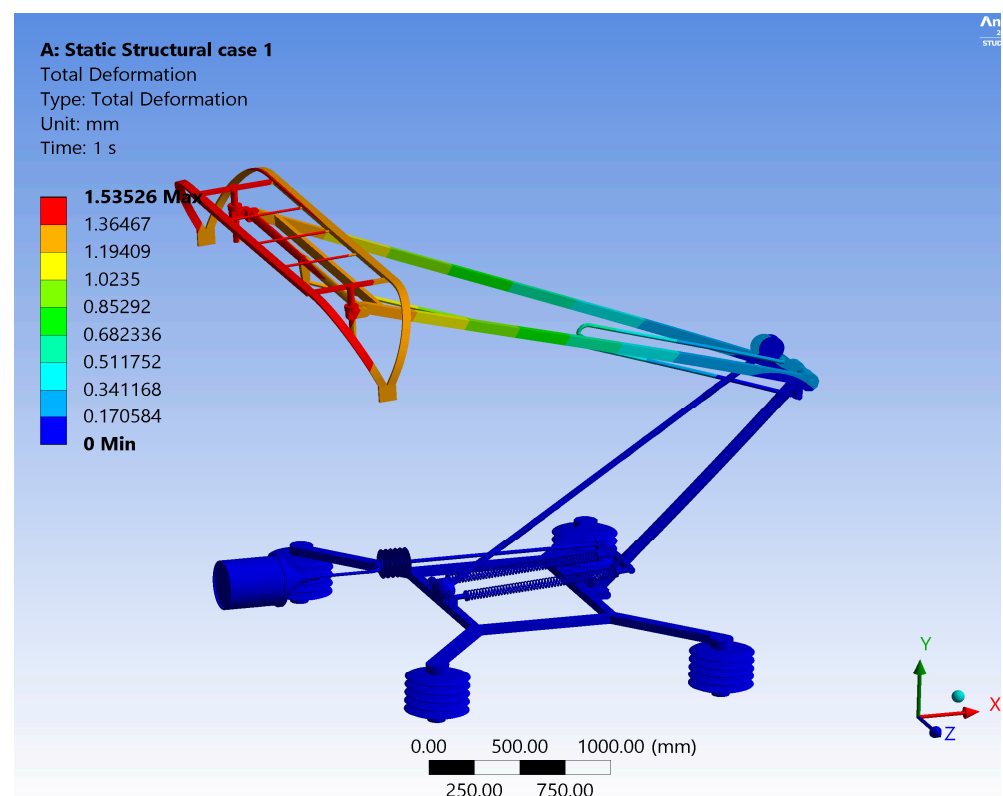


**Figure 6.** Total deformation distribution plot obtained on the cast-iron pantograph.

### 3.3. Strain Energy Distribution in the Cast-Iron Material

In Figure 7, the strain energy distribution plot sheds light on the areas of higher strain energy storage within the cast-iron pantograph.

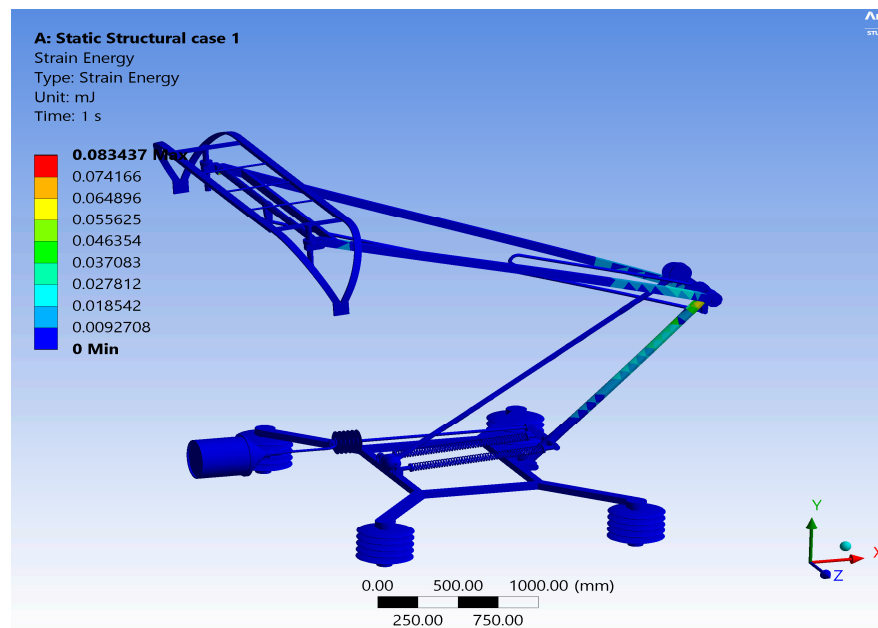


**Figure 7.** Strain energy plot of cast-iron pantograph.

Notably, the intersection of the lower arm and upper frame exhibits significant strain energy accumulation. The maximum strain energy recorded through the analysis is 0.083 mJ, demonstrating the energy-absorbing capabilities of the material in this specific region. Similar to equivalent stress, the strain energy maintains a consistent distribution across other areas of the pantograph.

### 3.4. Equivalent Stress Distribution in P100/AZ91C Mg MMC Pantograph

Moving on to the Al MMC pantograph, Figure 8 showcases its equivalent stress distribution plot. Mirroring the cast-iron pantograph, it highlights a prominent magnitude of equivalent stress at the intersection point of the upper frame and the drawbar.

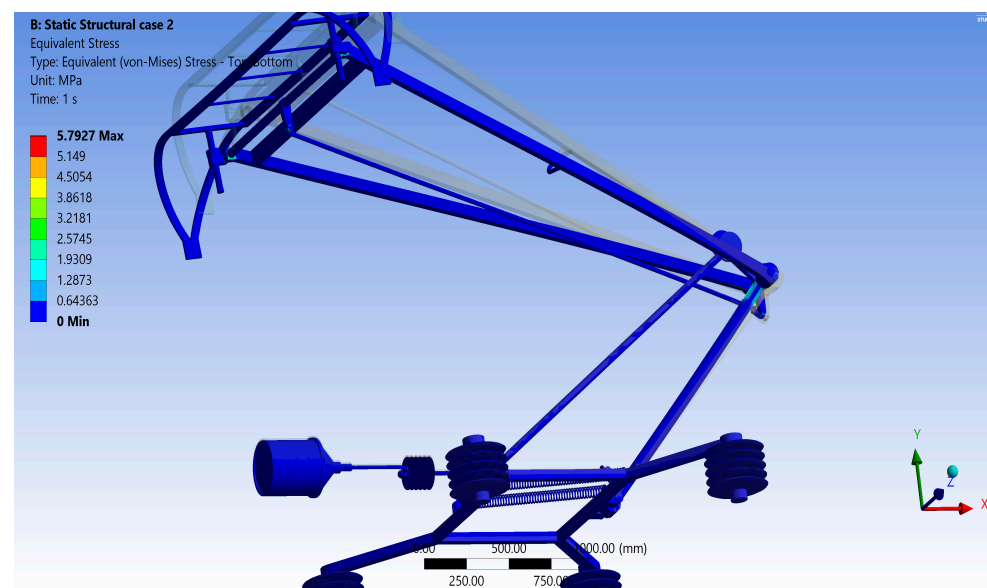


**Figure 8.** Equivalent stress distribution plot obtained on P100/AZ91C Mg MMC pantograph.

The maximum equivalent stress for the P100/AZ91C Mg MMC pantograph is 5.792 MPa. Just like its counterpart, the equivalent stress distribution shows uniformity in regions represented by the calming blue hues.

### 3.5. Total Deformation in P100/AZ91C Mg MMC Pantograph

Figure 9 presents the total deformation plot for the P100/AZ91C Mg MMC pantograph, demonstrating its remarkable mechanical response. The analysis reveals that the maximum deformation occurs on the pantograph slide, with a magnitude of 0.422 mm, visually emphasized by the prominent, red-colored region. This minimal deformation underscores the sturdiness of the Al MMC pantograph under loading conditions.

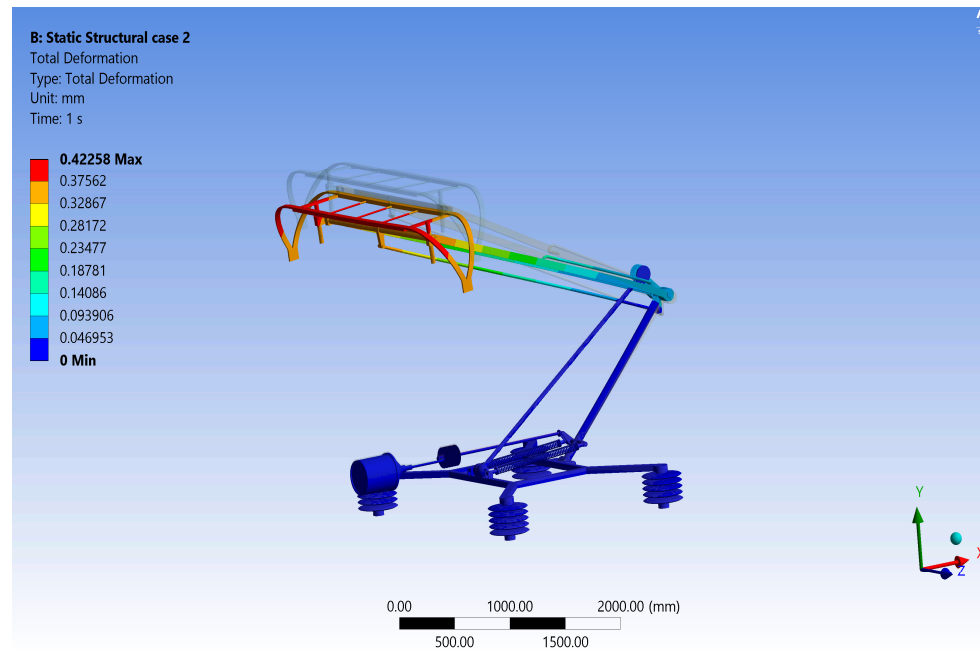


Figure 9. Total deformation distribution obtained on P100/AZ91C Mg MMC pantograph.

### 3.6. Strain Energy Distribution in P100/AZ91C Mg MMC Pantograph

Figure 10 explores the strain energy distribution plot for the P100/AZ91C Mg MMC pantograph. Here, similar to its cast-iron counterpart, higher strain energy is observed at the intersection of the lower arm and upper frame.

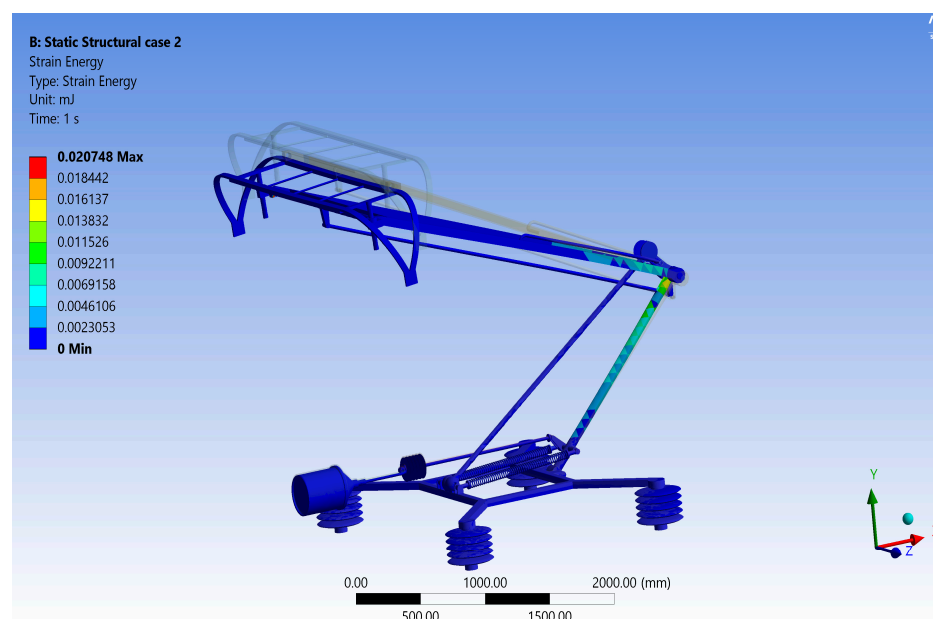


Figure 10. Strain energy plot obtained on P100/AZ91C Mg MMC pantograph.

The maximum strain energy recorded is 0.0207 mJ, confirming the strain-absorbing characteristics of the P100/AZ91C Mg MMC material in this region, with uniform energy distribution in other areas.

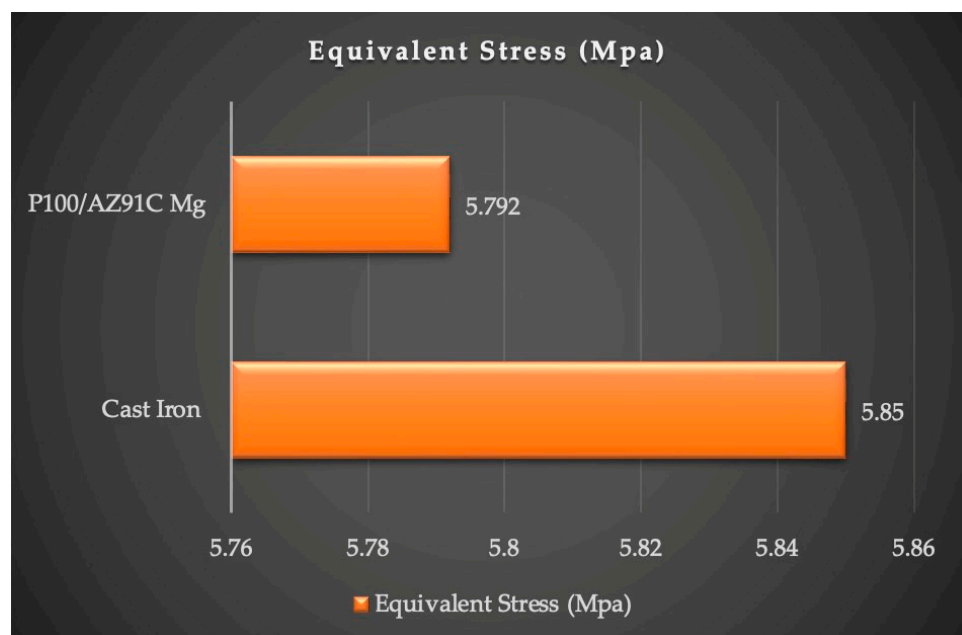
### 3.7. Comparison of Equivalent Stress and Deformation

Table 3 provides a comprehensive comparison of the equivalent stress and deformation for the two types of pantographs, summarizing the key findings. Notably, the pantograph made of Al MMC material has a lower mass compared to conventional cast-iron material. The mass of the Al MMC pantograph is 31.92% lower than the cast-iron pantograph.

**Table 3.** Comparison of data.

Material	Equivalent Stress (MPa)	Deformation (mm)	Strain Energy (mJ)	Mass (kg)
Cast Iron	5.85	1.59	0.083	127.926
P100/AZ91C Mg MMC	5.792	0.422	0.020	87.080

Further enriching our exploration, Figure 11 presents the Equivalent Stress Comparison Chart. Here, we observe a fascinating aspect—the P100/AZ91C Mg MMC pantograph exhibits lower equivalent stress levels when compared to its cast iron counterpart, opening the doors to a plethora of potential applications.



**Figure 11.** Equivalent stress comparison chart.

In Figure 12, the Deformation Comparison Chart takes the spotlight, showcasing an intriguing narrative. The deformation levels encountered in the P100/AZ91C Mg MMC pantograph are significantly lower when juxtaposed with the cast-iron pantograph. This stark contrast holds the promise of enhanced structural integrity and performance.

Finite element analysis has provided crucial insights into the mechanical behavior of our two pantograph materials: cast iron and P100/AZ91C Mg MMC. The stress distribution, deformation, and strain energy plots have revealed compelling details. Notably, the Al MMC pantograph exhibits a lower equivalent stress of 5.792 MPa compared to the cast-iron pantographs, which have an equivalent stress of 5.85 MPa. This slight reduction in equivalent stress bodes well for the future performance of these structures. This value is particularly low for the Al MMC pantograph, with a maximum deformation of 0.422 mm,

compared to its counterparts made from cast iron, which have up to 1.59 mm deformation. Considering this decrease, it means that it could possess enhanced stiffness and mechanical stability, which implies that the material could be used potentially in transportation systems. With regards to strain energy stored in these materials, it can be deduced that there are wide margins between them, with Al MMC having a value of 0.02 mJ, while aluminum has 0.083 mJ, as shown in Figure 13.



Figure 12. Deformation comparison chart.

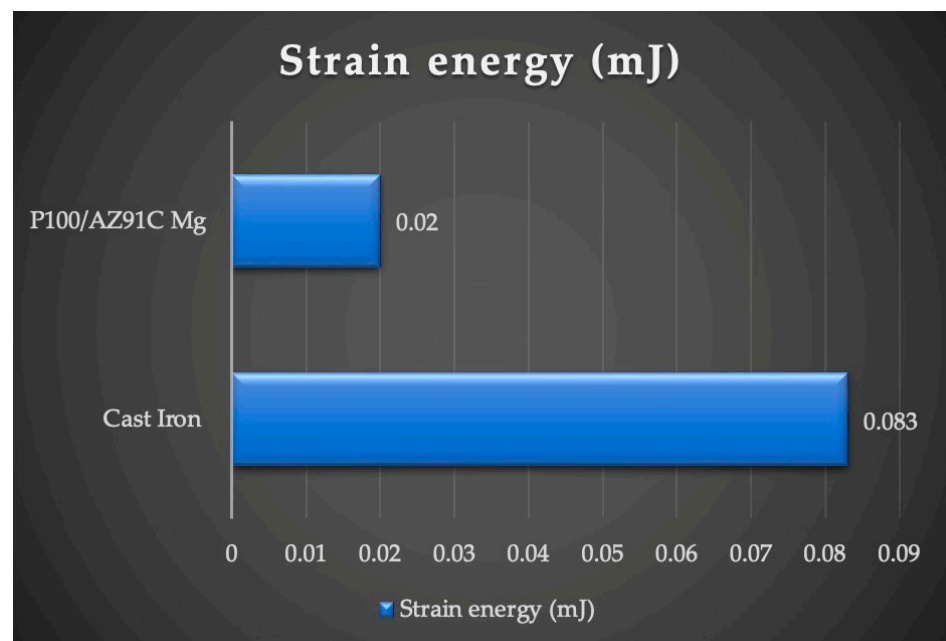


Figure 13. Strain energy comparison chart.

Such findings reveal that Al MMC is more resilient and better at accommodating mechanical stresses while, at the same time, saving energy. It is worth noting that the pantograph fabricated with Al MMC material is significantly lighter compared to the conventionally used cast-iron material. It is noted that the weight of the Al MMC pantograph

is decreased by 31.92% with respect to its cast-iron equivalent. This substantial mass reduction highlights its exceptional mechanical properties and positions it as an ideal material for lightweight applications in pantograph construction.

The resulting decrease in weight not only enhances structural efficiency but also promotes cost-effectiveness in system design and operation, which is a crucial aspect of system design. This finding underscores Al MMC's value in developing lightweight and cost-effective pantographs. The outcome of this study suggests a new era in pantograph technology, where Al MMC may become a leading material choice, enhancing the strength and efficiency of transport systems. Comparatively, Al MMC could lead to better structural performance if its equivalent stress, strain energy storage, and deformation are anything to go by, hence, making strides toward innovative and dependable transport systems.

#### 4. Conclusions

In the relentless pursuit of enhancing the structural integrity and performance of pantographs within transportation systems, this study harnessed the unique power of finite element analysis to explore the intricate landscape of pantograph behavior when subjected to static loading conditions.

The investigation not only revealed the core regions of the pantograph but also encouraged us into an innovation era through Al MMC material, a milestone to revolutionize transportation systems in terms of efficiency and sturdiness.

Substantial findings that emerged from this study are:

- **Reduced equivalent stress:** this is clearly seen in the reduction in equivalent stress by a surprising 0.18% due to Al MMC material, particularly P100/AZ91C Mg alloy introduction within pantographs. This is not just a number; it is also an important step toward ensuring that pantographs are powerful and efficient.
- **Saving energy:** the P100/AZ91C Mg MMC alloy not only eliminates stress but it also reduces strain energy by 63 J. The implication is that efficiency could be enhanced and more environment-friendly transport could pave the way.
- **Lightweight applications and cost-effectiveness:** the use of Al MMC material enabled the reduction in mass of the pantograph by 31.92% as compared to cast iron.

But this journey extends beyond these attainments, as the study successfully addressed the research questions that guided the inquiry:

1. The comparative study of the mechanical properties of MMC materials revealed their superiority compared to other conventional materials, hence marking a significant evolution in material science.

2. Examination of how MMC materials impact the strength, performance, and structural integrity of pantographs under varying loading conditions revealed a pathway to increased durability and efficiency, signifying a crucial development in transportation engineering.

3. The study used a quantitative approach, giving special attention to the comparison of equivalent stress, deformation, mass, and strain energy to gain some mechanical insights into the possible advantages and disadvantages of using MMC as a material in the design of the pantograph. This precise information could help make sound decisions regarding weight for future pantograph designs.

MMC products present features such as good mechanical properties, light structure, and improved durability of the pantograph equipment. In particular, the good mechanical behavior of the materials resulted in high reliability and efficiency. Despite that, the existing constraints, such as manufacturing challenges, higher material costs, and limited industrial comfort, underscore the need for appropriate measures and approaches to ensure successful adoption in practical applications.

4. The ability to compare directly MMC-based pantographs and their traditional counterparts in operation under operational stresses signifies a profound innovation serving the future development of transportation. Being aware of the inherent limitations, this study

emphasizes the mechanical aspects of pantograph operation through the simplification of models and FEA simulations.

Although effective in addressing its objectives, this study does not capture the wider complexities of real-life transport systems, including operational factors that are constantly changing. This targeted attention to mechanical detail provides a starting point for future research that considers wider functional patterns, opening up an interesting line of development. Analyzing these complex dynamics could require a separate study of the interaction between aerodynamics [25], electrical dynamics, and system-level interactions [26].

It underscores the pivotal role of innovative materials and methodologies in reshaping the future of transportation systems. This study not only demonstrates the potential of Al MMC but also initiates a new era in the transportation industry. The reductions in equivalent stress and strain energy are clear indicators of this material's extraordinary capabilities. Insight into future investigation could enable us to move closer to safer, more efficient, and innovation-driven transportation systems. This research aligns to the relentless quest for excellence in transportation engineering. The dynamic behavior of pantographs subjected to harmonic and transient forces could be targeted for future research.

**Author Contributions:** Conceptualization, A.A. and M.I.; methodology, M.I.; software, A.A.; validation, A.A. and M.I.; formal analysis, A.A.; investigation, A.A. and M.I.; resources, A.A.; data curation, M.I.; writing—original draft preparation, M.I.; writing—review and editing, A.A.; visualization, M.I.; supervision, A.A. and M.I.; project administration, M.I.; funding acquisition, M.I. All authors have read and agreed to the published version of the manuscript.

**Funding:** This research received no external funding and the APC was funded by the University of South Africa.

**Data Availability Statement:** Data are contained within the article.

**Conflicts of Interest:** The authors declare no conflicts of interest.

## References

1. Mei, G.; Luo, Q.; Qiao, W.; Huang, Z.; Lu, J.; Wang, J. Study of Load Spectrum Compilation Method for the Pantograph Upper Frame Based on Multi-Body Dynamics. *Eng. Fail. Anal.* **2022**, *135*, 106099. [[CrossRef](#)]
2. Ouyang, M.; Chen, S.; Li, Q.; Yang, Z. Numerical Investigation on Aerodynamic Forces and Flow Patterns of High-Speed Trains from Open Air into Long Tunnel. *J. Wind Eng. Ind. Aerodyn.* **2022**, *229*, 105142. [[CrossRef](#)]
3. Wu, G.; Dong, K.; Xu, Z.; Xiao, S.; Wei, W.; Chen, H.; Li, J.; Huang, Z.; Li, J.; Gao, G.; et al. Pantograph–Catenary Electrical Contact System of High-Speed Railways: Recent Progress, Challenges, and Outlooks. *Railw. Eng. Sci.* **2022**, *30*, 437–467. [[CrossRef](#)]
4. Zvolenský, P.; Leštinský, L.; Ďungel, J.; Grenčík, J. Pantograph Impact on Overall External Noise of a Railway Vehicle. *Transp. Res. Procedia* **2021**, *55*, 661–666. [[CrossRef](#)]
5. Liu, Z.; Wang, H.; Chen, H.; Wang, X.; Song, Y.; Han, Z. Active Pantograph in High-Speed Railway: Review, Challenges, and Applications. *Control Eng. Pract.* **2023**, *141*, 105692. [[CrossRef](#)]
6. Zhou, N.; Cheng, Y.; Zhang, X.; Zhi, X.; Zhang, W. Wear Rate and Profile Prediction of Cu-Impregnated Carbon Strip for High-Speed Pantograph. *Wear* **2023**, *530–531*, 205056. [[CrossRef](#)]
7. Fomin, O.; Prokopenko, P.; Kara, S.; Píšťek, V.; Kučera, P. Study of the Basic Criteria of the Pantograph and Overhead Line Interaction in Operating Conditions. *Results Eng.* **2023**, *19*, 101336. [[CrossRef](#)]
8. Wang, J.; Mei, G. Effect of Pantograph's Main Structure on the Contact Quality in High-Speed Railway. *Shock Vib.* **2021**, *2021*, 4037999. [[CrossRef](#)]
9. Shimanovsky, A.; Yakubovich, V.; Kapliuk, I. Modeling of the Pantograph–Catenary Wire Contact Interaction. *Procedia Eng.* **2016**, *134*, 284–290. [[CrossRef](#)]
10. Yang, J.; Song, Y.; Lu, X.; Duan, F.; Liu, Z.; Chen, K. Validation and Analysis on Numerical Response of Super-High-Speed Railway Pantograph–Catenary Interaction Based on Experimental Test. *Shock Vib.* **2021**, *2021*, 9922404. [[CrossRef](#)]
11. Tripathiutkarsh, L.; Sandeepgiri, T.; Singh, M. Pantograph Engraving Machine—A Review. *Int. J. Mech. Prod. Eng.* **2018**, *6*, 1–4.
12. Vilas Barpate, N.; Thakur, S.N.; Kshetre, P.S.; Wankhede, P.A. Design and Development of a Portable Pantograph for Engraving Letters on Wood. *Int. J. Sci. Res. Dev.* **2016**, *4*, 384–387.
13. Morris, J.; Robinson, M.; Palacin, R. Use of Dynamic Analysis to Investigate the Behaviour of Short Neutral Sections in the Overhead Line Electrification. *Infrastructures* **2021**, *6*, 62. [[CrossRef](#)]
14. Zdziebko, P.; Martowicz, A.; Uhl, T. An Investigation into Multi-Domain Simulation for a Pantographcatenary System. *ITM Web Conf.* **2017**, *15*, 03001. [[CrossRef](#)]

15. Wu, Z.; Xie, Z.; Wang, P.; Ding, W. Aerodynamic Drag Performance Analysis of Different Types of High-Speed Train Pantograph Fairing. *J. Appl. Sci. Eng.* **2020**, *23*, 509–519. [[CrossRef](#)]
16. Sidorov, O.A.; Goryunov, V.N.; Salya, I.L.; Tomilov, V.V. Dynamic Models Choice for Pantographs of High-Speed Railway Transport. In Proceedings of the 2016 Dynamics of Systems, Mechanisms and Machines (Dynamics), Omsk, Russia, 15–17 November 2016; IEEE: Piscataway, NJ, USA, 2016; pp. 1–4.
17. Song, D.; Jiang, Y.; Zhang, W. Dynamic Performance of a Pantograph–Catenary System with Consideration of the Contact Surface. *Proc. Inst. Mech. Eng. Part F J. Rail Rapid Transit* **2018**, *232*, 262–274. [[CrossRef](#)]
18. Agarwal, A.; Mthembu, L. Structural Analysis and Optimization of Heavy Vehicle Chassis Using Aluminium P100/6061 Al and Al GA 7-230 MMC. *Processes* **2022**, *10*, 320. [[CrossRef](#)]
19. Agarwal, A.; Mthembu, L. Investigation of Dynamic Factors in Different Sections of HVC by Static and Free Vibration Modal Analysis. *Ann. De Chim. Sci. Des Matériaux* **2022**, *46*, 75–84. [[CrossRef](#)]
20. Agarwal, A.; Mthembu, L. Design and Response Surface Optimization of Heavy Motor Vehicle Chassis Using P100/6061 Al MMC. In *Recent Advances in Materials and Modern Manufacturing*; Palani, I.A., Sathya, P., Palanisamy, D.P., Eds.; Springer: Singapore, 2022; pp. 1–12.
21. Rawal, S. Metal-Matrix Composites for Space Applications. *JOM J. Miner. Met. Mater. Soc.* **2001**, *53*, 14–17. [[CrossRef](#)]
22. ANSYS Library File. Available online: <https://www.ansys.com/content/dam/amp/2021/august/webpage-requests/education-resources-dam-upload-batch-2/material-property-data-for-eng-materials-BOKENGEN21.pdf> (accessed on 1 February 2024).
23. Marumo, R.; Agarwal, A.; Mthembu, L. Material Optimization of Robotic Arm Using FEM and Rigid Body Dynamics. In *Recent Advances in Materials and Modern Manufacturing: Select Proceedings of ICAMMM 2021*; Springer: Singapore, 2022; pp. 789–801.
24. Qian, W.J.; Chen, G.X.; Zhang, W.H.; Ouyang, H.; Zhou, Z.R. Friction-Induced, Self-Excited Vibration of a Pantograph-Catenary System. *J. Vib. Acoust.* **2013**, *135*, 051021. [[CrossRef](#)]
25. Jackson, F.F.; Mishra, R.; Rebelo, J.M.; Santos, J.; Antunes, P.; Pombo, J.; Magalhães, H.; Wills, L.; Askill, M. Modelling Dynamic Pantograph Loads with Combined Numerical Analysis. *Railw. Eng. Sci.* **2023**, *32*, 81–94. [[CrossRef](#)]
26. Zhang, M.; Yin, B.; Sun, Z.; Bai, Y.; Yang, G. A Feasibility Study on Applying Meta-Heuristic Optimization and Gaussian Process Regression for Predicting the Performance of Pantograph-Catenary System. *Acta Mech. Sin.* **2024**, *40*, 523282. [[CrossRef](#)]

**Disclaimer/Publisher’s Note:** The statements, opinions and data contained in all publications are solely those of the individual author(s) and contributor(s) and not of MDPI and/or the editor(s). MDPI and/or the editor(s) disclaim responsibility for any injury to people or property resulting from any ideas, methods, instructions or products referred to in the content.